Nearly-free electronlike surface resonance of a β-Si_3N_4(0001)/Si(111)-8 × 8 interface

R. Flammini,[1,*] P. Allegrini,[2] F. Wiame,[3] R. Belkhou,[4] F. Ronci,[1] S. Colonna,[1] D. M. Trucchi,[5] F. Filippone,[5] S. K. Mahatha,[6,7] P. M. Sheverdyaeva,[7] and P. Moras[7]

[1]*CNR-ISM Istituto di Struttura della Materia, Via del Fosso del Cavaliere 100, I-00133 Roma, Italy*

[2]*CNR-IFN Istituto di Fotonica e Nanotecnologie, Via Cineto Romano 42, I-00156 Roma, Italy*

[3]*Institut de Recherche de Chimie Paris (CNRS - Chimie ParisTech), Ecole Nationale Supérieure de Chimie de Paris (ENSCP), 11 rue Pierre et Marie Curie, F-75005 Paris, France*

[4]*Synchrotron SOLEIL, L'Orme des Merisiers, Saint-Aubin, B.P. 48F, F-91192 Gif Sur Yvette, France*

[5]*CNR-ISM Istituto di Struttura della Materia, Via Salaria km 29.300, I-00019 Monterotondo Scalo (RM), Italy*

[6]*International Center for Theoretical Physics (ICTP), I-34014 Trieste, Italy*

[7]*CNR-ISM, Istituto di Struttura della Materia, Area Science Park, S.S. 14, km 163.5, I-34149 Trieste, Italy*

(Received 30 October 2014; revised manuscript received 22 January 2015; published 9 February 2015)

We report the discovery of a nearly-free electronlike resonant state for a β-Si_3N_4(0001)-8 × 8 layer grown on Si(111), as observed by angle-resolved photoemission and scanning tunneling spectroscopy. Comparison with measurements performed on a Si(111)-7 × 7 surface helped us in the identification of the band. It is found that this parabolic state is degenerate with surface projected bulk bands of the Si(111) substrate.

DOI: 10.1103/PhysRevB.91.075303 PACS number(s): 73.20.At, 77.55.df, 79.60.Bm, 71.20.−b

I. INTRODUCTION

Heterointerfaces in electronic devices are usually not abrupt and are a source of defects [1]. As an exception, it is known that epitaxial β-Si_3N_4(0001) films can be obtained on silicon, owing to a favorable lattice correspondence: the 2 × 2 cell of the Si(111) surface almost perfectly matches the 1 × 1 cell of β-Si_3N_4(0001) [2–4]. Ultrathin layers of epitaxial silicon nitride can also be grown [5] showing, at the same time, the ability to prevent the formation of silicides. Indeed, studies reporting on the interaction of this nitride layer with Au, Co, and Fe (among the most reactive elements with silicon) [6–10], demonstrated this ability at temperatures up to 600 K [8,11]. This is of paramount importance as metal/Si(111) ideal interfaces can now be produced without the drawbacks of the formation of interface states due to silicides. Recently epitaxial β-Si_3N_4(0001) films grown on Si(111) have been also suggested to be ideal substrates to preserve the high mobility properties of graphene [12] and silicene [13].

This system was studied theoretically as well as experimentally since the first evidence of crystalline growth [14]. Most part of the theoretical studies focused on the atomic structure and on the electronic structure of the nitride/silicon interface [3,4,15], even very recently [16]. While several attempts to describe the atomic structure of the reconstructed surface exist in the literature [17–21], studies about its electronic structure have been probably hampered by the high computational demand. According to the currently accepted model [17] the basic system consists of a rest layer of silicon and nitrogen atoms in a very complex relaxed bulk-terminated structure and an adlayer formed by nine nitrogen atoms per surface unit cell. The diamond shaped unit cell is asymmetric: only one-half of the cell shows three pairs of atoms in between the nitrogen adatoms. However, problems regarding the details of the reconstruction are not yet solved, e.g., the existence of dangling bonds (DBs), the kinds of DBs, and the differences between simulations and scanning tunneling microscopy (STM) measurements [18,19,22–25].

As for the surface electronic structure, the experimental studies are limited to integrated band structures recorded at photon energies larger than 100 eV [7,26–28] except for the paper by Tokumitsu *et al.* [29] in which angle-resolved photoemission (ARPES) measurements at 32.5 and 45 eV photon energy, were reported: the authors identified the N 2p and Si 3p and 3s bands at binding energies larger than 4.5 eV, ascribing the unusual band structure to the umklapp process occurring at the interface between silicon and nitride. In 2003, Kim *et al.* [26] claimed that a feature appearing in the valence band taken at 134 eV, 1.1 eV below the Fermi level, would be related to the 8 × 8 reconstruction. However, this evidence has not been confirmed so far [7,27,28]. Indeed, at present a clear spectroscopic signature of the 8 × 8 reconstructed β-Si_3N_4(0001) layer has not yet been reported.

In this respect, we report here the evidence for a resonance along the $\bar{\Gamma}\bar{K}$ and $\bar{\Gamma}\bar{M}$ high symmetry directions of the surface Brillouin zone (SBZ) of the 8 × 8-reconstructed surface. Such an electronic state has been identified by ARPES and scanning tunneling spectroscopy (STS). The ARPES results are compared to the ones recorded on Si(111)-7 × 7 in order to unravel its peculiar band structure. The experimental spectra have been compared with density functional theory (DFT) calculations, and the surface resonance is suggested to be related to the 8 × 8 reconstruction.

II. EXPERIMENT

Si(111) samples were cut from p-type (B-doped) silicon wafers with resistivity $\rho \simeq 0.005\ \Omega$cm. The surface was outgassed at 700 K for several hours using direct resistive heating. The sample was cleaned by repeated flashes of several seconds at 1520 K at a base pressure of $\sim 3 \times 10^{-10}$ mbar, leading to a sharp 7 × 7 low-energy electron diffraction (LEED) pattern. The 7 × 7-reconstructed surface was held at a temperature of approximately 1050 K and exposed to 10^2 langmuirs of NH_3. This ensured the growth of two bilayers

*Roberto.Flammini@cnr.it

of silicon nitride [26]. No evidence of atomic segregation was recorded, as verified by core level photoemission spectroscopy.

ARPES spectra were recorded at the VUV Photoemission Beamline (Elettra, Italy). The spectra were acquired at room temperature (RT) at photon energies ranging from 40 to 120 eV, using a Scienta R-4000 electron analyzer. The total energy and angular resolution were set to 15 meV (40 eV photon energy) and 0.3°, respectively. The Fermi levels were measured on the metallic 7×7-reconstructed Si(111) surface [30]. This was done systematically upon flashing the nitrided surface at high temperature to restore the 7×7 reconstruction. Data handling routines were run on the rough data to subtract the background and to work out the second-derivative spectra, in order to extract the relevant information.

The STM measurements were carried out in constant current mode at RT using an Omicron LT scanning tunneling microscope housed in an ultrahigh vacuum (UHV) chamber (5×10^{-11} mbar base pressure). Electrochemically etched tungsten tips were used after a cleaning procedure by electron bombardment. The reported bias voltage (V_S) is relative to the sample.

Silicon nitride in the β phase has a hexagonal close-packed (HCP) lattice structure. The in-plane and out-of-plane lattice constants are $a = b = 7.604$ Å and $c = 2.906$ Å [31]. Silicon has a face-centered cubic (FCC) diamond structure with a lattice parameter $a = 5.43$ Å. Hence, β-Si_3N_4(0001) and Si(111) show a hexagonal SBZ, although the stacking sequence of the atomic layers is different. In this regard, it is noted that while the $\bar{\Gamma}\bar{M}$ and $\bar{\Gamma}\bar{M}'$ in a FCC lattice are not equivalent (being surface projections of nonequivalent L and X points of bulk reciprocal space), in a HCP lattice the two symmetry directions are indeed equivalent. Therefore, only spectra along the $\bar{\Gamma}\bar{K}$ and $\bar{\Gamma}\bar{M}$ high symmetry directions are here considered. In the Fig. 1, the SBZs of Si(111) and β-Si_3N_4(0001) are shown as orange and blue hexagons, respectively. For β-Si_3N_4(0001), the crystallographic directions and the sizes of $\bar{\Gamma}\bar{K}$ and $\bar{\Gamma}\bar{M}$ are $\langle 10\bar{1}0\rangle$ 0.55 Å^{-1} and $\langle 11\bar{2}0\rangle$ 0.48 Å^{-1}, respectively. Extension of the SBZ beyond the first zone along the $\bar{\Gamma}\bar{K}$ direction allows us to probe the $\bar{K}\bar{M}$, whose size is 0.27 Å^{-1}. As for the Si(111) substrate, the size of the SBZ is almost twice the one of silicon nitride.

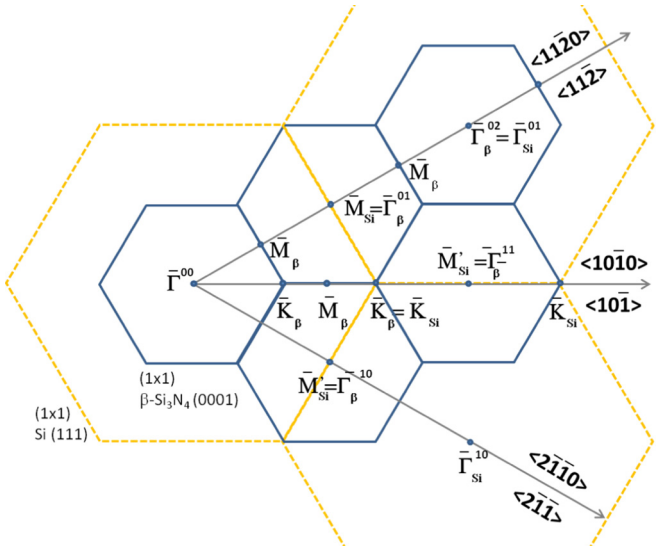

FIG. 1. (Color online) Reciprocal space of the β-Si_3N_4(0001) and Si(111) (1×1) surface. SBZs are identified as blue solid and orange dashed hexagons, respectively. The subscripts Si and β refer to silicon and silicon nitride, respectively. Grey solid lines indicate the high symmetry directions along which the ARPES measurements have been performed.

III. COMPUTATIONAL TECHNIQUE

The simulations were performed using a plane waves density functional approach, as implemented in the QUANTUM ESPRESSO suite of programs [32], with the Perdew-Burke-Ernzerhof [33] gradient correction and van der Waals interactions [34–38]. We used Vanderbilt ultrasoft pseudopotentials [39], and 30 and 180 Ry kinetic energy cutoffs for electronic wave functions and density, respectively. The supercell is hexagonal, 2×2 with respect to the bulk truncated Si(111), corresponding to a 1×1 supercell of β-Si_3N_4, and with ≈18 Å vacuum space added along z to simulate the surface. A $3 \times 3 \times 1$ **k**-point Monkhorst-Pack mesh was used for geometry optimizations, while a $6 \times 6 \times 1$ mesh was used for the potential to be diagonalized in the band dispersion calculation. We saturated the lower Si (111) surface with H atoms, accounting for 84 atoms for all the supercells. We considered for our simulations only the 1×1 surface of β-Si_3N_4 instead of the β-Si_3N_4 8×8 reconstruction in order to keep computational demand as low as possible.

We optimized the bulk lattice parameter for both Si and β-Si_3N_4. The Si lattice parameter found is equal to 3.87 Å, in good agreement with experimental data ($5.83/\sqrt{2} = 3.84$ Å). The calculated surface density is 7.71×10^{14} cm^2. We obtained for bulk β-Si_3N_4 $a = 7.67$ Å and $c/a = 0.3819$, and a indirect energy gap of $E_g = 4.24$ eV, in line with experimental and theoretical data [24,27,40–42]. From the present data, we immediately note the tiny lattice mismatch (<1%) between the β-Si_3N_4 lattice parameter and twice that of Si(111).

IV. RESULTS

A. Experiment

Figure 2 shows the band structure of the β-Si_3N_4(0001)/Si(111)-8×8 interface measured at RT along the $\bar{\Gamma}\bar{K}\bar{M}\bar{K}$ and $\bar{\Gamma}\bar{M}\bar{\Gamma}$ lines. The measurement was carried out at 40 eV photon energy, i.e., in surface sensitive conditions. At the $\bar{\Gamma}$ point, two bands labeled B and S are noted. While the band B, pointing downward (holelike), can be tentatively assigned to the bulk band of the silicon substrate [43], the S band is unknown. This upward (electronlike) band disperses along the $\bar{\Gamma}\bar{K}$ as well as the $\bar{\Gamma}\bar{M}$ direction with the same curvature, showing a minimum at $\bar{\Gamma}$ at about 2.20 eV below the Fermi level.

In order to gain an insight into the assignment of the bands, we performed the same measurements on the bare 7×7-reconstructed Si surface.[1] The ARPES spectra taken at 40 eV are shown in Fig. 3. No evidence of the S band is

[1]The nitrided surface was flashed up 1500 K in order to restore the 7×7 reconstruction. No nitrogen was present on the substrate and no contamination from other elements was detected by photoemission.

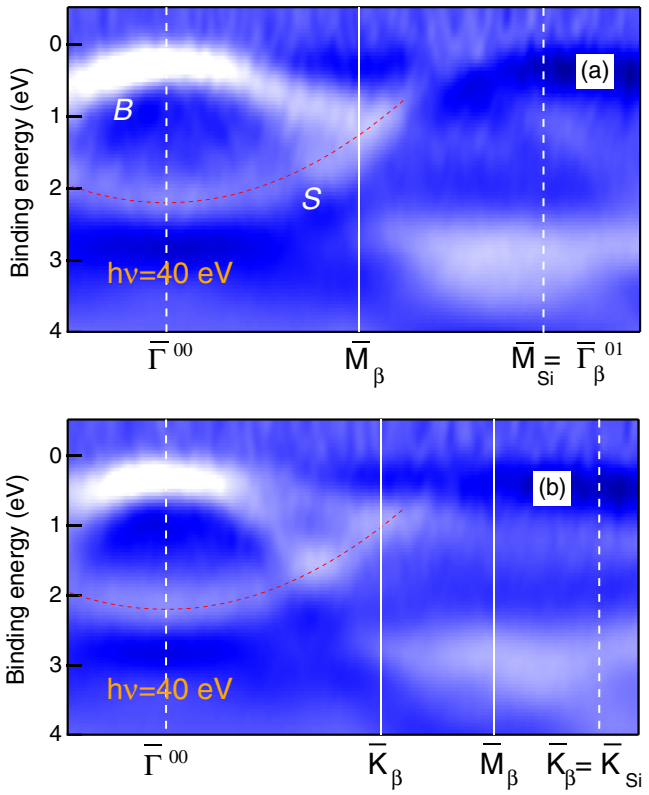

FIG. 2. (Color online) ARPES spectra recorded on the β-Si_3N_4(0001)-8 × 8 surface, along (a) the $\bar{\Gamma}\bar{M}$ and (b) the $\bar{\Gamma}\bar{K}$ high symmetry directions (see Fig. 1). Photon energy $h\nu = 40$ eV. Vertical solid and dashed lines refer to the (1 × 1) SBZs of β-Si_3N_4(0001) and Si(111), respectively. High symmetry directions are labeled for the two SBZs. The B and S stand for the bulk and surface bands, respectively. The dashed red line represents the best fit to the data indicating the surface band S. The ARPES images show some intensity above the Fermi level: this is clearly an artifact and must not be considered.

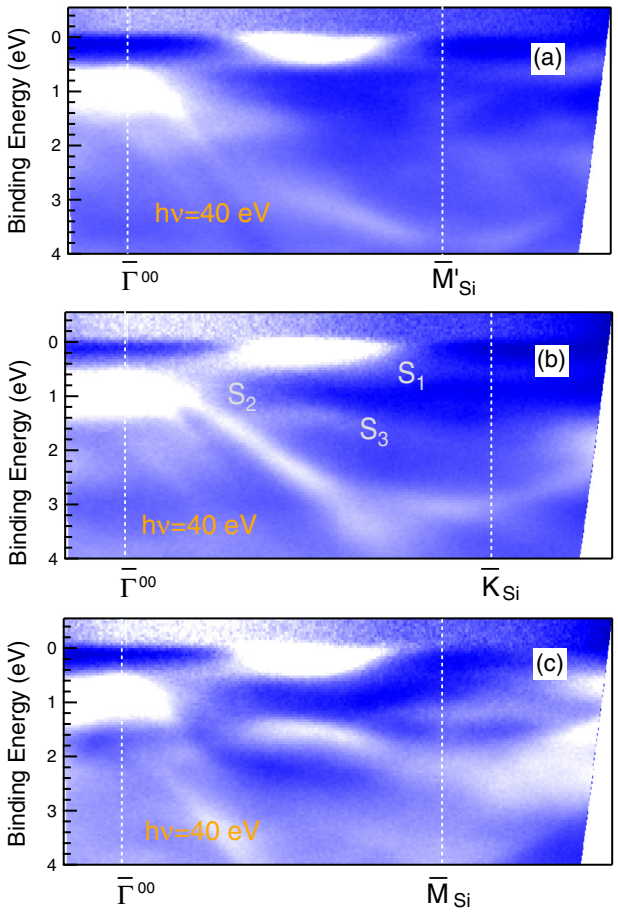

FIG. 3. (Color online) ARPES spectra recorded on the Si(111)-7 × 7 surface, along (a) the $\bar{\Gamma}\bar{M}'$, (b) the $\bar{\Gamma}\bar{K}$, and (c) $\bar{\Gamma}\bar{M}$ high symmetry directions (see Fig. 1). Photon energy $h\nu = 40$ eV. Vertical dashed lines refer to the (1 × 1) SBZ of the Si(111). The labels S_1, S_2, and S_3 refer to the surface states of Si(111)-7 × 7.

recorded: this is why the band is attributed to the presence of the nitride layer. At variance with the nitrided surface, a clear Fermi level is detected at about half the distance $\bar{\Gamma}\bar{M}'$, $\bar{\Gamma}\bar{K}$, and $\bar{\Gamma}\bar{M}$ in panels (a), (b) and (c), respectively, in correspondence with the 7 × 7 surface state S_1, generally attributed to adatoms [30].

One of the requirements for a genuine surface state to exist is the independence of the dispersion curve (E vs $k_\parallel$) on the photon energy. This is clearly demonstrated in Fig. 4, where several spectra recorded along the $\bar{K}\bar{\Gamma}\bar{K}$ direction at different photon energies are shown. In the figure, although with different intensity, the same curvature for the nitride S state was recorded for all the spectra, as the one measured at 40 eV (Fig. 2). The red dashed lines represent the best fit to the data, returning a parabola with $\frac{m^*}{m_0} = 0.96$, where m^* and m_0 are the effective and free electron masses, respectively. We note the absence of the nitride state for photon energies larger than 100 eV. At variance with the band S, the bands pointing downwards show a clear variation of the curvature as a function of the photon energy: this is a further demonstration of their Si bulk origin.

The absence of the nitride S band in Fig. 4 for large photon energies cannot be ascribed to the difference in the inelastic mean free path for electrons of different kinetic energy, as only a few Å of difference exist [44]. In contrast, the most important effect is the cross section of the N $2p$, electrons which is reduced by 17 times in passing from 35 to 135 eV photon energy [45], and of the Si $3s$ and Si $3p$ electrons, losing about 4 times their intensity in the same photon energy range. In this respect, a feature reported in the photoemission valence band taken at 134 eV photon energy was previously ascribed to the presence of a surface state [26]. However, that intense peak at a binding energy of −1.1 eV was never measured afterwards [7,27–29]. Our data also cannot support that experimental evidence mainly on two grounds: on the one hand, angular resolved photoemission is needed to highlight the tiny feature (which is hidden if integrated in all the

The surface reconstruction was verified by LEED. This allowed us to compare directly the two surfaces, exploiting the same spatial orientation and the same energy reference. The Fermi level was measured on the 7 × 7 surface by using the well known metallicity of the adatoms at RT (see for example Losio *et al.* [30]).

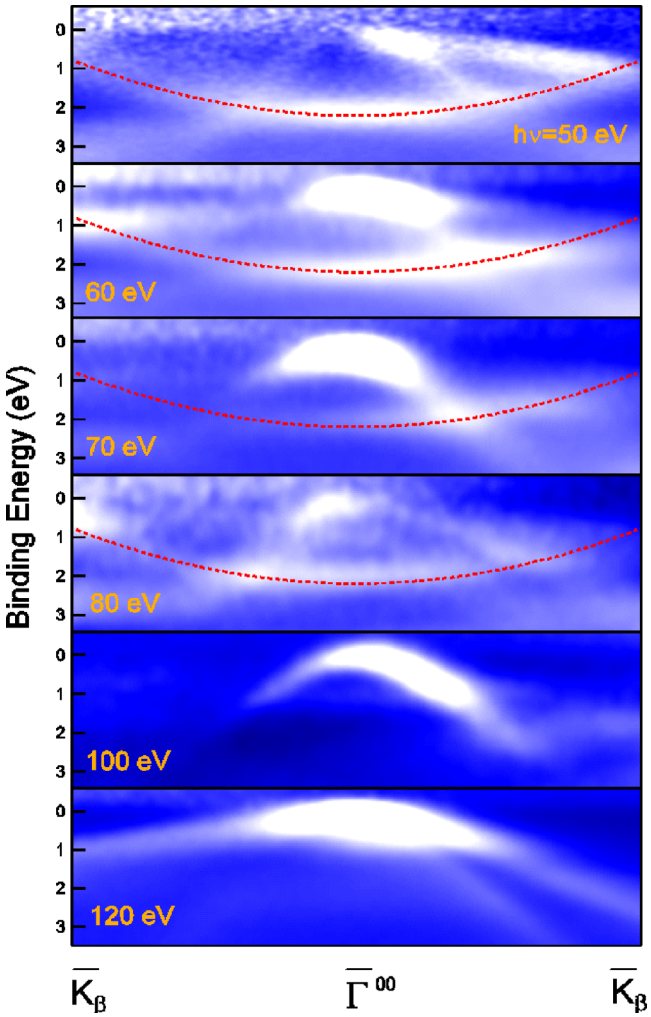

FIG. 4. (Color online) Photon energy dependence of the state *S* (see text). The red dashed line represents the best fit to the experimental data shown in Fig. 2(b). Above 100 eV, the band disappears due to the decrease of the cross section of the N $2p$ states (see text).

directions of the outgoing electrons); on the other hand, the choice of the photon energy is crucial due to the variation of the cross section.

In Fig. 5 constant-current STM images of the β-Si_3N_4(0001) surface and the corresponding STS spectrum are shown. In particular, Fig. 5(a) exhibits a reconstructed 8×8 surface in which the bright protrusions do not fully occupy all the available adsorption sites. Generally these features are attributed to N adatoms (located at an average distance of about 1 nm [17,23,24]). This enables us to clearly detect the underlying β-Si_3N_4(0001) relaxed bulk structure [17]. This is better shown in panel (b), where we display a high resolution image of the green highlighted area in panel (a), collected immediately after the first one. Interestingly, we noted that some bright protrusions suddenly disappeared while the image was scanned,[2] indicating a high surface mobility of nitrogen adatoms. Such a behavior is further proven by a direct comparison of two consecutive images, as highlighted by the green ovals showing the appearance (disappearance) of two nitrogen adatoms, with a solid line (dashed line), respectively. This is also confirmed by the STM images of Ref. [17]. Figure 5(c) displays a STM image collected in another region of the sample surface, in which a more complete adlayer is present. In this case, we did not observe evidence for nitrogen mobility, most probably because of the lower number of vacancies through which the adatoms can diffuse. In the most accepted model of the 8×8 reconstruction [17], in one half of the unit cell three additional pairs of atoms between the N adatoms are predicted. As seen in Fig. 5, there is no evidence for that, even if the spatial resolution is higher than the one in the literature [17]. Beside, in panel (d) the comparison between the ARPES profile and STS spectrum is shown. The ARPES line profile is extracted from the rough data corresponding to Fig. 2(a) at the point $\bar{\Gamma}$; apart from the well known peak sitting at 4.2 eV below the Fermi energy (attributed to the N $2p$ states), it shows a shoulder ranging between -2 and -3 eV, corresponding to the band *S* recorded in the ARPES images. The STS spectrum was obtained from a 30×30 nm^2 image [in part shown in panel (c)], by averaging all the normalized differential conductance curves $(\frac{dI}{dV})/(\frac{I}{V})$ recorded at each point of a grid formed by 80×80 points, with an interpoint distance of 0.1 nm. The agreement between tunneling and photoemission spectroscopies is then demonstrated by the peak centered at about -2.2 eV as well as a signal increase above -3.8 eV, generally attributed to the N adatoms.

B. Theoretical model

In order to simulate the structure of the interface, we added two unit cells of β-Si_3N_4 on top of the Si(111) supercell along the (0001) direction, i.e., 28 atoms for a total nitride thickness of $\approx$6 Å [26]. The atomic arrangement suggested in Ref. [16] is shown in Fig. 6, where we note the N atom saturating the DBs of silicon atoms within the Si(111) surface (see arrow). The resulting electronic band dispersion is reported in Fig. 7, in close agreement with that obtained by Flage-Larsen *et al.* [16]. The band splitting, however, is not replicated here. This is due to the arrangement of the different layers in the simulations. Indeed, Flage-Larsen *et al.* performed a bulk simulation with two β-Si_3N_4/Si interfaces, while we used just one interface, simulating a surface rather than a bulk. The other difference is the presence of flat states in the conduction band between $\bar{K}$ and $\bar{M}$ high symmetry points; such states originate from unsaturated orbitals belonging to surface atoms, as they are wiped off when the surface is saturated with H atoms [13].

It is interesting to note that the top of the valence band is located at the $\bar{M}$ point. Projecting such a state onto atomic orbitals, it is found that it can be attributed to atoms belonging to both sides of the interface. On the other hand, such states at $\bar{\Gamma}$ belong to the silicon atoms on the Si(111) side of the system, in agreement with the proposed assignment to the top of the bulk silicon valence band. Our calculations suggest that the states lying between 0 and -1 eV binding energy range can be attributed to interface states, while those below -1 eV correspond to bulk silicon states, in accord with the literature [16].

[2]The tip scanned from left to right, moving from the bottom to the upper part of the scanned area.

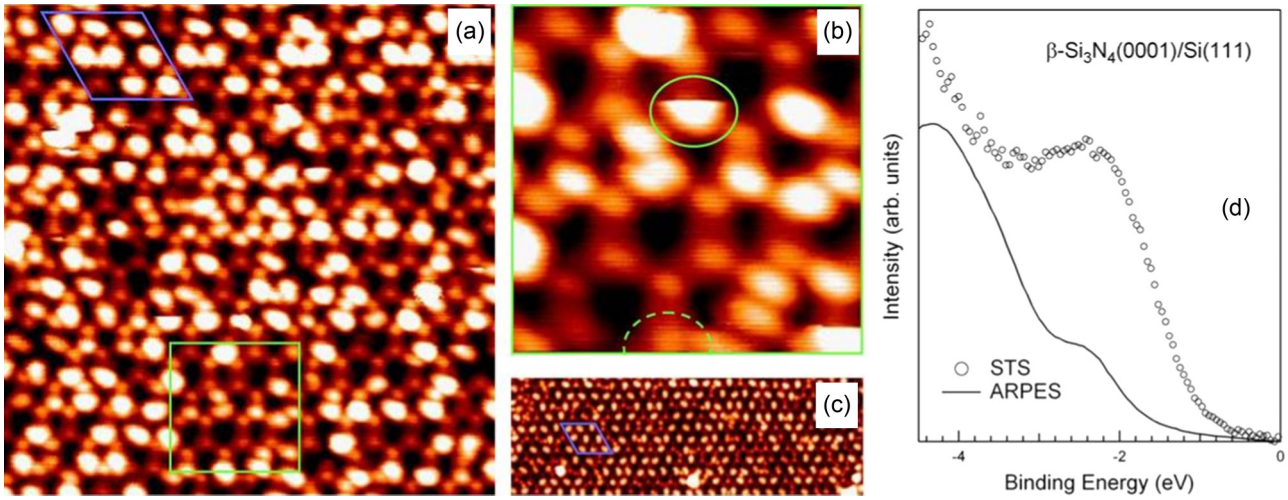

FIG. 5. (Color online) (a) 15×15 nm^2 STM image ($V_S = -4$ V, $I_T = 2$ nA) of a β-Si_3N_4/Si(111) sample. (b) High resolution 4×4 nm^2 STM image ($V_S = -4$ V, $I_T = 2$ nA) collected immediately after the one in panel (a) on the sample area highlighted by a green square. Green ovals highlight mobility of nitrogen adatoms (see text for discussion). (c) 10×30 nm^2 STM image ($V_S = -4$ V, $I_T = 2$ nA) showing the almost complete 8×8 reconstruction. The blue lozenge highlights the 8×8 unit cell. (d) Comparison between the STS spectrum and the ARPES line profile at Γ, taken from the rough data corresponding to Fig. 2(a). The STS spectrum is obtained from the image in panel (c); see text. The STS and ARPES profiles are not in scale.

V. DISCUSSION

The new band S measured in Fig. 2 is attributed to the presence of the nitride layer. Its behavior as a function of the photon energy clearly suggests a two-dimensional origin, as no dependence on $k_\perp$ was recorded. However, due to the thinness of the nitride layer, this state can be ascribed to the surface as well as to the interface atoms.[3] Turning to the calculations, we discover that the S band lies in the binding energy range where the bulk bands of the simulated system are located. Therefore, the S band cannot arise from the interface atoms. Moreover, one of the criteria to ascribe a band to a surface state is to grow an adsorbate and induce new bonds affecting the nature of the surface. To that purpose, another experiment (whose results will be published elsewhere) was performed by exposing the 8×8 surface to molecular oxygen, confirming the participation of the topmost atoms to the surface band. This is why we are more ready to assign the S band to the surface atoms.

Figure 7 shows the superposition of the experimental data with the theoretical calculations. The light grey shaded area corresponds to the surface projected bulk bands of the Si(111) sample, adapted from Ref. [46]. In order to demonstrate that S is an actual surface state, it has to be compared with the surface projection of the bulk states. In this respect, due to the thinness of the nitride layer, only the Si(111) bulk states are relevant. With such an assumption, we see that the S band is degenerate with the bulk states, so that the band actually corresponds to a surface resonance.

The parabola describing the band shows a nearly free electron behavior as the mass ratio is $\simeq 1$; this is interesting because an arrangement of the atoms at a distance of about 1 nm (as in the case of the nitrogen adatoms in the 8×8 reconstruction) is more compatible with a flat surface band where the superposition of the valence orbitals is negligible (as a comparison, the bulk terminated nitride surface unit cell is 7.61 Å). Indeed, this is what happens for the adatom DBs of Si(111)-7×7, where the electrons are mostly localized on the p_z vertical orbitals (far apart, 7.68 Å [47]) and the associated band shows no dispersion (state S_1 of Fig. 3). At variance, in

[3]Of the two grown bilayers of silicon nitride, we consider that one is involved in the surface reconstruction, while the other one participates in the interface with silicon; this is why the *bulk* of the silicon nitride is not taken into consideration.

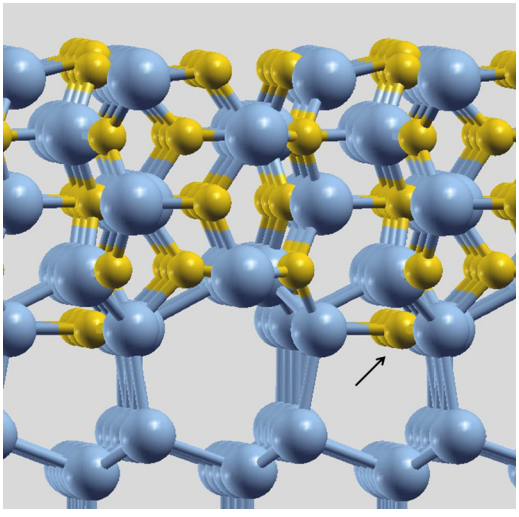

FIG. 6. (Color online) Ball and stick model of the β-Si_3N_4(0001)/Si(111) interface. Orange and blue balls represent nitrogen and silicon atoms, respectively. Nitrogen atoms are present in the topmost layer of the silicon substrate (see arrow) saturating the DBs at the interface and energetically stabilizing all of the structure (see text).

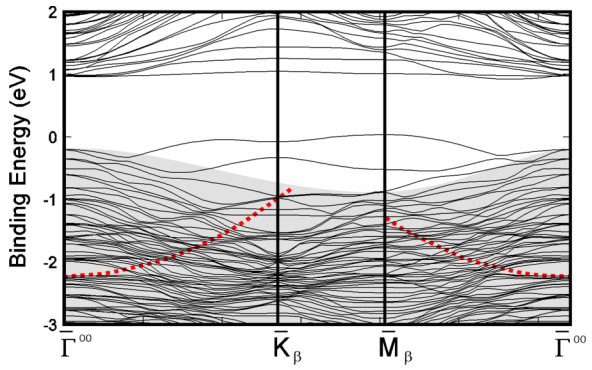

FIG. 7. (Color online) Comparison between theoretical calculations and experimental spectra. The electronic band structure corresponds to the interface model displayed in Fig. 6. The red dashed line represents the best fit to the experimental data indicating the surface resonance band *S*. The light grey shaded area shows the surface projected bulk bands of the Si(111) sample. The binding energy is arbitrarily aligned to the experimental Fermi level.

our case, the *S* band must be related to a well defined lattice such as that of the bulk-relaxed structure [identified below the bright protrusion of Fig. 5(a)], where the average distance among the atoms is much less than 1 nm. Even the model of Bermudez [21], which performed an energy relaxation of the bulk terminated surface, cannot account for the *S* band. According to the author, the occupied surface state (π-bonding character) derived mainly from the three terminal N atoms (i.e., bonded to only two silicon atoms and hosting one DB) gives rise to a holelike band, in contrast to our findings.

The presence of a feature at -4.2 eV binding energy, measured in the photoemission [26,28] or STS [17,24,40] spectra due to the N 2p states, cannot be related directly to the surface reconstruction: this feature is predicted to exist even in thick layers of crystalline [48] or amorphous silicon nitride [49] and is not due exclusively to N atoms of the reconstructed surface. In our opinion, the band *S* is the actual signature of the surface reconstruction. However, at the moment, a definitive statement on the subject is impossible: a comprehensive understanding of the origin of the *S* band cannot yet be gathered without a full atomic simulation of the 8×8 reconstruction which, though very resource demanding, becomes now highly desirable.

In summary, beside the well known ability to passivate the silicon and preserve the electronic and magnetic properties of a metallic adsorbate, the nitride layer shows also a peculiar surface electronic band structure. This can pave the way to studies aiming at band tailoring for the exploitation of graphene-based and spin-based electronic devices.

VI. CONCLUSIONS

We report the observation of a nearly-free electron surface state for the β-Si_3N_4(0001)/Si(111)-8×8 system. The comparison with ARPES spectra recorded on Si(111)-7×7 allowed us to disentangle the surface band structure of the nitride layer. The ARPES and STS measurements complemented by DFT calculations show that the surface band is a resonance, being degenerate with the surface projected bulk bands of the Si(111) substrate.

ACKNOWLEDGMENTS

The research leading to these results has received funding from the European Community's Seventh Framework Programme (FP7/2007-2013) under Grant Agreement No. 312284.

[1] H. J. Queisser and E. E. Haller, Science **281**, 945 (1998).
[2] D. Messier and W. Croft, in *Preparation and Properties of Solid State Materials*, edited by W. R. Wilcox, Growth Mechanisms and Silicon Nitride, Vol. 7 (Marcel Dekker, New York, 1982), Chap. 2.
[3] G. L. Zhao and M. E. Bachlechner, Phys. Rev. B **58**, 1887 (1998).
[4] M. Yang, R. Q. Wu, W. S. Deng, L. Shen, Z. D. Sha, Y. Q. Cai, Y. P. Feng, and S. J. Wang, J. Appl. Phys. **105**, 024108 (2009).
[5] X. Shi, M. Shriver, Z. Zhang, T. Higman, and S. A. Campbell, J. Vac. Sci. Technol. A **22**, 1146 (2004).
[6] S. Gwo, C.-P. Chou, C.-L. Wu, Y.-J. Ye, S.-J. Tsai, W.-C. Lin, and M.-T. Lin, Phys. Rev. Lett. **90**, 185506 (2003).
[7] R. Flammini, R. Belkhou, F. Wiame, S. Iacobucci, and A. Taleb-Ibrahimi, Surf. Sci. **579**, 188 (2005).
[8] R. Flammini, F. Wiame, R. Belkhou, A. Taleb-Ibrahimi, C. Spezzani, P. Moras, and C. Crotti, J. Appl. Phys. **103**, 083528 (2008).
[9] K. Eguchi, Y. Takagi, T. Nakagawa, and T. Yokoyama, Phys. Rev. B **85**, 174415 (2012).
[10] K. Eguchi, Y. Takagi, T. Nakagawa, and T. Yokoyama, J. Phys. Conf. Ser. **430**, 012129 (2013).
[11] R. Flammini, F. Wiame, R. Belkhou, A. Taleb-Ibrahimi, and P. Moras, Surf. Sci. **606**, 1215 (2012).
[12] M. Yang, C. Zhang, S. Wang, Y. Feng, and Ariando, AIP Adv. **1**, 032111 (2011).
[13] F. Filippone, J. Phys. Condens. Matter **26**, 395009 (2014).
[14] A. J. V. Bommel and F. Meyer, Surf. Sci. **8**, 381 (1967).
[15] R. Sekine, H. Kataoka, S. Tokumitsu, K. Edamoto, and E. Miyazaki, Surf. Sci. **357**, 366 (1996).
[16] E. Flage-Larsen, O. M. Løvvik, C. M. Fang, and G. Kresse, Phys. Rev. B **88**, 165310 (2013).
[17] H. Ahn, C.-L. Wu, S. Gwo, C. M. Wei, and Y. C. Chou, Phys. Rev. Lett. **86**, 2818 (2001).
[18] Y. Morita and H. Tokumoto, Surf. Sci. **443**, L1037 (1999).
[19] G. Zhai, J. Yang, N. Cue, and X. Wang, Thin Solid Films **366**, 121 (2000).
[20] A. A. Bagatur'yants, K. P. Novoselov, A. A. Safonov, J. V. Cole, M. Stoker, and A. A. Korkin, Surf. Sci. **486**, 213 (2001).
[21] V. M. Bermudez, Surf. Sci. **579**, 11 (2005).
[22] X. Wang, G. Zhai, J. Yang, L. Wang, Y. Hu, Z. Li, J. C. Tang, X. Wang, K. K. Fung, and N. Cue, Surf. Sci. **494**, 83 (2001).
[23] S. Gwo, C.-L. Wu, F.-S. Chien, T. Yasuda, and S. Yamasaki, Jpn. J. Appl. Phys. **40**, 4368 (2001).

[24] C.-L. Wu, J.-L. Hsieh, H.-D. Hsueh, and S. Gwo, Phys. Rev. B **65**, 045309 (2002).
[25] E. Bauer, Y. Wei, T. Müller, A. Pavlovska, and I. S. T. Tsong, Phys. Rev. B **51**, 17891 (1995).
[26] J. W. Kim and H. W. Yeom, Phys. Rev. B **67**, 035304 (2003).
[27] H.-M. Lee, C.-T. Kuo, H.-W. Shiu, C.-H. Chen, and S. Gwo, Appl. Phys. Lett. **95**, 222104 (2009).
[28] V. M. Bermudez and F. K. Perkins, Appl. Surf. Sci. **235**, 406 (2004).
[29] S. Tokumitsu, T. Anazawa, K. Ozawa, E. Miyazaki, K. Edamoto, and H. Kato, Surf. Sci. **317**, 143 (1994).
[30] R. Losio, K. N. Altmann, and F. J. Himpsel, Phys. Rev. B **61**, 10845 (2000).
[31] Z. Zhang and U. Kaiser, Ultramicroscopy **109**, 1114 (2009).
[32] P. Giannozzi, S. Baroni, N. Bonini, M. Calandra, R. Car, C. Cavazzoni, D. Ceresoli, G. L. Chiarotti, M. Cococcioni, I. Dabo, A. Dal Corso, S. de Gironcoli, S. Fabris, G. Fratesi, R. Gebauer, U. Gerstmann, C. Gougoussis, A. Kokalj, M. Lazzeri, L. Martin-Samos, N. Marzari, F. Mauri, R. Mazzarello, S. Paolini, A. Pasquarello, L. Paulatto, C. Sbraccia, S. Scandolo, G. Sclauzero, A. P. Seitsonen, A. Smogunov, P. Umari, and R. M. Wentzcovitch, J. Phys. Condens. Matter **21**, 395502 (2009).
[33] J. P. Perdew, K. Burke, and M. Ernzerhof, Phys. Rev. Lett. **77**, 3865 (1996).
[34] M. Dion, H. Rydberg, E. Schröder, D. C. Langreth, and B. I. Lundqvist, Phys. Rev. Lett. **92**, 246401 (2004).
[35] T. Thonhauser, V. R. Cooper, S. Li, A. Puzder, P. Hyldgaard, and D. C. Langreth, Phys. Rev. B **76**, 125112 (2007).
[36] G. Román-Pérez and J. M. Soler, Phys. Rev. Lett. **103**, 096102 (2009).
[37] K. Lee, E. D. Murray, L. Kong, B. I. Lundqvist, and D. C. Langreth, Phys. Rev. B **82**, 081101 (2010).
[38] R. Sabatini, E. Kucukbenli, B. Kolb, T. Thonhauser, and S. de Gironcoli, J. Phys. Condens. Matter **24**, 424209 (2012).
[39] D. Vanderbilt, Phys. Rev. B **41**, 7892 (1990).
[40] C.-L. Wu, W.-S. Chen, and Y.-H. Su, Surf. Sci. Lett. **606**, L51 (2012).
[41] T. A. Pham, T. Li, S. Shankar, F. Gygi, and G. Galli, Phys. Rev. B **84**, 045308 (2011).
[42] M. Kumar, B. Roul, T. N. Bhat, M. K. Rajpalke, A. Kalghatgi, and S. Krupanidhi, Thin Solid Films **520**, 4911 (2012).
[43] J. Chelikowsky and M. L. Cohen, Phys. Rev. B **14**, 556 (1976).
[44] S. Tanuma, C. J. Powell, and D. Penn, Surf. Interface Anal. **43**, 689 (2011).
[45] J. J. Yeh and I. Lindau, At. Data Nucl. Data Tables **32**, 1 (1985).
[46] R. I. G. Uhrberg, G. V. Hansson, J. M. Nicholls, P. E. S. Persson, and S. A. Flodström, Phys. Rev. B **31**, 3805 (1985).
[47] S. Hasegawa, X. Tong, S. Takeda, N. Saito, and T. Nagao, Prog. Surf. Sci. **60**, 89 (1999).
[48] Y.-N. Xu and W. Y. Ching, Phys. Rev. B **51**, 17379 (1995).
[49] V. A. Gritsenko, Phys. Usp. **55**, 498 (2012).